Materials Today: Proceedings 45 (2021) 5829–5834

Contents lists available at ScienceDirect

Materials Today: Proceedings

journal homepage: www.elsevier.com/locate/matpr

Prediction models for bond strength of steel reinforcement with consideration of corrosion

Masoud Ahmadi [a], Ali Kheyroddin [b], Mahdi Kioumarsi [c,d,*]

[a] Department of Civil Engineering, Ayatollah Boroujerdi University, Boroujerd, Iran
[b] Department of Civil Engineering, Semnan University, Semnan, Iran
[c] Department of Civil Engineering and Energy Technology, OsloMet –Oslo Metropolitan University, Pilestredet 35, 0166, Oslo, Norway
[d] Faculty of Engineering, Østfold University College, Halden, Norway

ARTICLE INFO

Article history:
Available online 2 April 2021

Keywords:
Corrosion
Prediction model
Steel reinforcement
Bond strength
Artificial neural networks

ABSTRACT

Corrosion phenomena is one of the main deterioration causes, which remarkably affects the behavior of structural reinforced concrete (RC) members in seismic regions. Researches on reducing rehabilitation cost, performance assessment, and accurate modelling of corrosion-affected RC structures are progressively becoming popular in recent years. Corrosion diminishes bond capacity between reinforcement and surrounding concrete, which induces reduction in strength and ductility of members. The aim of this investigation is to provide a prediction approach based on a large number of results from published researches related to corroded reinforcement in concrete members using artificial neural networks (ANN). The minimizing mean square error criterion and increasing regression value of predicted results are considered for evaluation of training performance of ANN models. The validity of proposed model is checked using collected experimental database. Results show that estimated model has acceptable agreement with experimented data.

1. Introduction

Based on the design codes and guidelines, strain in steel reinforcement of reinforced concrete (RC) elements should be the same as that in the adjacent concrete. In other words, bond between concrete and reinforcement helps reinforcement to have same strain with surrounding concrete [1]. The bond strength depends on the friction condition between steel and concrete, which could have significant effects on the performance of RC structures [2]. Aggressive environment, as one of the main reasons of corrosion, may result in a large deterioration of RC structural elements and consequently decreases their bond strength. Corrosion could affect the serviceability and durability of the RC structures and generate remarkable maintenance costs [3–5]. Uniform and pitting are two types of corrosion in RC members [5]. Carbonation is the main source of uniform corrosion, which can cause concrete cover cracking, loss in bond strength and anchorage between concrete and reinforcements [6–8]. When a reinforcement is corroded, the iron oxides form the expanded products in the steel–concrete interfacial zone. This expansion results in internal pressure around the reinforcement, which leads to cracking, spalling of concrete and thereby reduces rebar confinement [9,10]. Corrosion degrades rib height and diminishes cross-sectional area of rebar which affects the interaction between concrete and ribs of rebars, ultimate capacity, and failure mode [11–13]. For the above-mentioned reasons, it is crucial to better understand and characterize the effects of reinforcement corrosion on the deterioration of interfacial bond capacity between reinforcement and adjacent concrete.

Although finite element is one of the appropriate methods to investigate the global behavior of the corroded RC structures and other composite structure [14–17] but recently there has been particular attention to the application of soft commuting methods such as artificial neural networks (ANN) for the assessment of residual capacity of RC structures [18,19]. The present study proposed a new approach to estimate the average value of bond capacity between corroded reinforcement and surrounding concrete by gathering wide range of experimental results using ANN method. The results of this study could utilize directly to improve modelling and assessing of existing RC structures with considering corrosion effects.

* Corresponding author.
E-mail address: mahdik@oslomet.no (M. Kioumarsi).

https://doi.org/10.1016/j.matpr.2021.03.263
2214-7853/

2. Background

Up to now, many investigations have been done to explain the effects of corrosion on the bond-slip behavior between the reinforcement and concrete in RC structures. Furthermore, some analytical, empirical, and numerical bond models are proposed for determining the residual bond strength between concrete and corroded reinforcement [20–28]. Cabrera [24] proposed an equation to predict the bond loss based on cracks pattern, rate of corrosion, and corrosion intensity using experimental data. Coronelli [22] studied the effect of different confinement situations and roles of the interface pressure of corroded steel reinforcement on residual bond strength. Wang and Liu [25] studied the degradation of bond strength and suggested a simple theoretical bond approach to determine the effect of corrosion on decreasing of bond capacity before and after corrosion cracking.

The *fib* model codes [29] proposed four-stage bond equations for monotonic loading, see Fig. 1. The suggested bond model can be calculated as a function of the slip between reinforcement and adjacent concrete:

$$\tau = \begin{cases} \tau_{max}\left(\frac{s}{s_1}\right)^{\alpha} & 0 \le s \le s_1 \\ \tau_{max} & s_1 \le s \le s_2 \\ \tau_{max} - (\tau_{max} - \tau_r) * \frac{s-s_2}{s_3-s_2} & s_2 \le s \le s_3 \\ \tau_r & s_3 \le s \end{cases} \quad (1)$$

where, τ_{max} is maximum bond stress (without corrosion), τ_r define as residual bond stress, and other parameters of local bond stress-slip bond expression are determined using *fib* model code [29] for pull-out failure mode based on good or all other conditions.

Wu and Zhao [21], to resolve difficulties in computational simulations of concrete structures such as incompletely and discontinuity of existing models and non-convergence of numerical simulations, proposed a single and mathematically continuous bond-slip relationship (Eqs. 2–8) for splitting and pull-out failures. This model can used for plain and confined concrete.

$$\tau = \frac{\tau_{max}}{\left[e^{-B\ln\frac{\frac{B}{D}}{B-D}} - e^{-D\ln\frac{\frac{B}{D}}{B-D}}\right]}\left(e^{Bs} - e^{Ds}\right) \quad (2)$$

$$\tau_{max} = \frac{2.5}{1 + 3.1e^{-0.47K}} * \sqrt{f_c'} \quad (3)$$

$$K_{co} = \frac{C}{d_b} \quad (4)$$

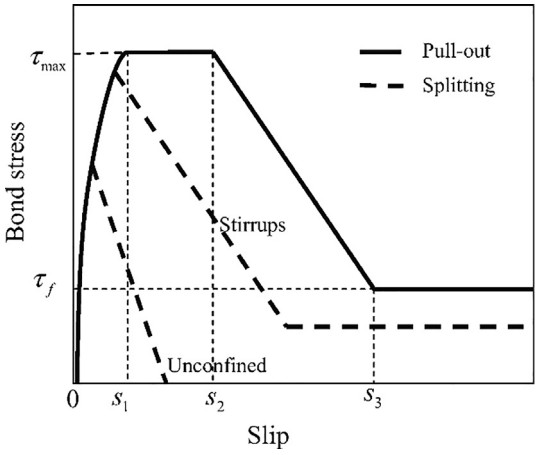

Fig. 1. Local bond stress-slip model [8].

$$K_{st} = \frac{A_{st}}{nS_{st}d_b} \quad (5)$$

$$K = K_{co} + 33K_{st} \quad (6)$$

$$B = \frac{0.0254 + K_{st}}{-0.0232 - 8.34K_{st}} \quad (7)$$

$$D = 3\ln\left(\frac{0.7315 + K}{5.176 + 0.3333K} - 0.13\right) - 3.375 \quad (8)$$

where, K_{co}, K_{st} and K are coefficients to consider the influence of concrete confinement, stirrups confinement, and effect of combined confinement, respectively. B and D are coefficients, controlling the post-peak softening slope and the slope of the ascending branch of stress–strain diagram, A_{st} is the cross-sectional area of all legs of transverse reinforcement, s and S_{st} are slip and stirrup spacing, respectively.

3. Experimental database

In order to predict the average interfacial bond stress among corroded reinforcement and concrete, large number of experimental results were gathered from the previous studies [23,30–38]. All of the bars in the database were deformed bars where corrosion occurred after casting of concrete. The loading condition was monotonic tension and all the results obtained from pull-out test.

In general, the various parameters effect on the bond strength between concrete and reinforcement. Among them, the major factors are bar size and its location in cross section of concrete member, concrete cover, confinement (effect of stirrups) witch delay the spalling of concrete, compressive strength of concrete, length of reinforcement, and corrosion level (minor, moderate and extensive).

Using some parts of the gathered data, the change of relative bond capacity (R_t) versus corrosion level (ψ) is plotted in equations (9) and (10) and Fig. 2. In these equations, ψ is utilized to evaluate the corrosion level as percentage loss of weight.

$$\psi = \frac{W_0 - W}{W_0} * 100 \quad (9)$$

$$R_t = \frac{\tau(\psi)}{\tau_{max}(\psi = 0)} \quad (10)$$

Statistical details of the mechanical-geometric characteristics of the collected database are presented in Table 1. The considered parameters include bar diameter (d_b), ratio of bar diameter to embedment length ($\frac{d_b}{l}$), ratio of clear cover to bar diameter ($\frac{c}{d_b}$), yielding strength of reinforcement (f_y), compressive strength of concrete (f_c'), and corrosion level (ψ).

4. Bond strength model

4.1. Artificial neural networks

Artificial Neural Networks (ANNs) is an efficient approach in intricate engineering problems. Up to now, ANN has utilized in many practical civil engineering problems such as axial capacity estimation of composite column [39–41], shear strength estimation of RC beams [42–44], and compressive strength of concrete [45–47]. The feed forward-back propagation state of multilayer network is one of the efficient type of neural networks, which is utilized in many research works. The network contains consecutive layers of neurons, and appropriate transfer functions as efficient tools to determine the intricate relationships between targets

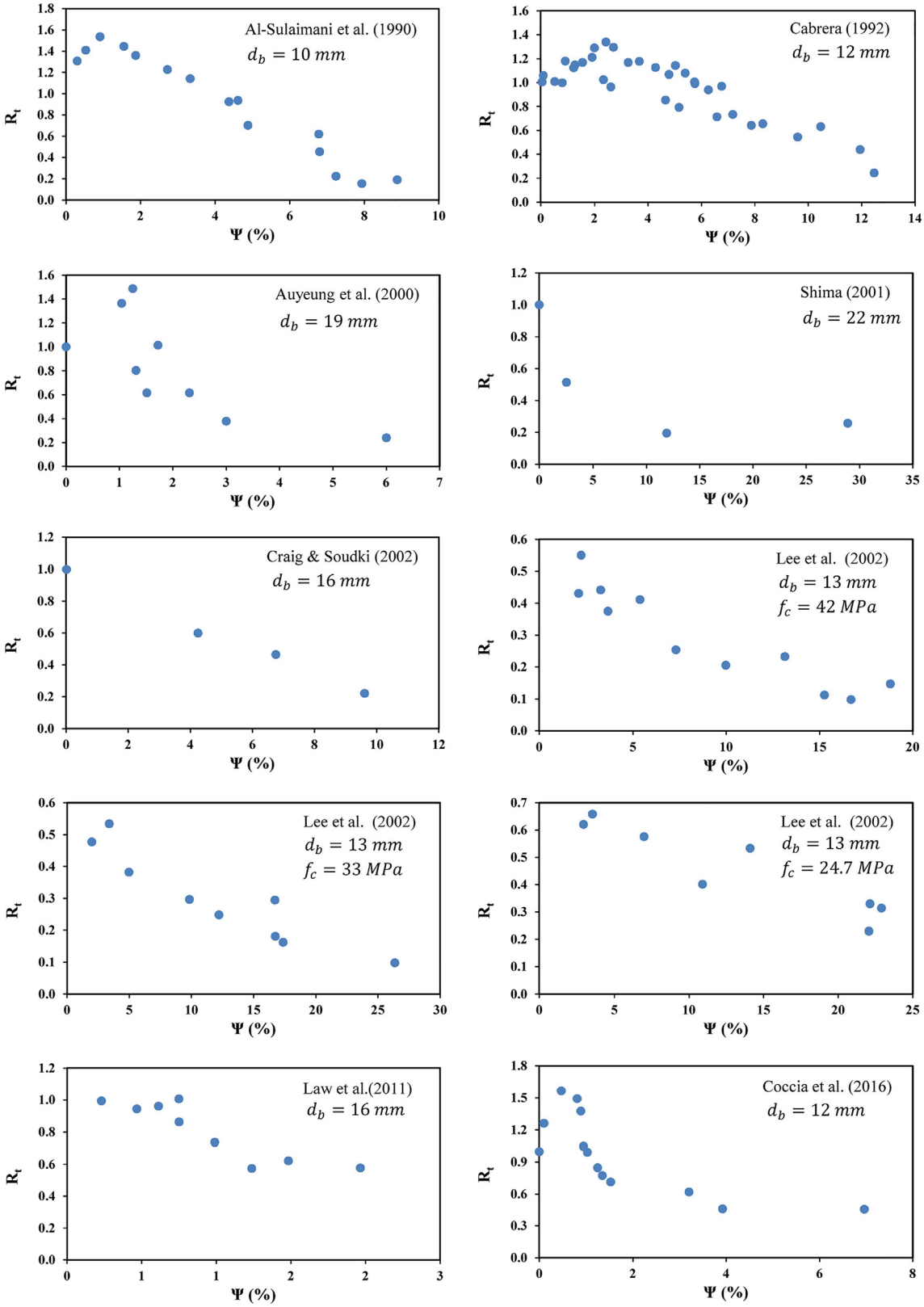

Fig. 2. Change of bond capacity at different corrosion levels.

and input variables [48]. The Levenberg–Marquardt (LM) algorithm, which is an efficient technique among training algorithm, is used in this study. LM method is an iterative procedure which is widely used as a learning algorithm in non-linear least squares problems [48]. However, a LM training back propagation network is used to predict bond capacity of steel reinforcement with consideration of corrosion.

LM procedure randomly divides input and output vectors of data into three categories: training, verification and testing. By applying a trial and error method to obtain optimum performance,

Table 1
The statistical details of collected experimental data.

	d_b(mm)	$\frac{d_b}{l}$	$\frac{c}{d_b}$	f_y(MPa)	$f_c^{'}$(MPa)	ψ(%)
Min	10	0.04	1.0	315	24.40	0.0
Max	25	0.25	7.50	606	56	28.9
Mean	16.14	0.16	4.26	419.3	37.3	4.43
Standard deviation	4.95	0.07	1.90	56.04	10.5	4.93
Coefficient of variation	0.31	0.41	0.45	0.13	0.28	1.11

the percent of training, verification, and test sets are considered as 60%, 20%, and 20%. The training part was utilized to regulate the weights and biases. The validation data controlled network to prevent overtraining phenomena. Related error to validation set starts to heighten when overtraining occurs. An over-trained system has poor estimative efficiency. For more certainty, the testing set was utilized to check the accuracy of trained networks using new data.

4.2. Proposed model

Key parameters in creation of ANN are selection number of hidden layers and number of neurons in them. In the present paper, one hidden layer was utilized and number of neurons in hidden layer were varied between 5 and 14 and finally the best number was used in proposed ANN-model. Two criteria were utilized for stopping the training procedure, which are Regression values (R-values), and Mean Square Error (MSE). Lower MSE value (Eq. (11)) and upper value of R (Eq. (12)) mean better performance of the ANN-model.

$$MSE = \frac{1}{n}\sum_{i=1}^{n}(\tau_{calc.} - \tau_{test})^2 \tag{11}$$

$$R^2 = 1 - \frac{\sum_{i=1}^{n}(\tau_{calc.} - \tau_{test})^2}{\sum_{i=1}^{n}(\tau_{calc.})^2} \tag{12}$$

The MSE and R-values of the created ANN-models versus various number of neurons in hidden layer are illustrated in Figs. 3 and 4, respectively.

Based on the obtained results in Figs. 3 and 4, the ANN-approach with five number of nodes in hidden layer was chosen as efficient network. The configuration of optimum ANN-model is shown in Fig. 5.

The matrix for weights and biases related to ANN-model in the hidden and output layers are as follows:

$$Weight_{hidden} = \begin{bmatrix} -1.0633 & -0.42121 & 0.03481 & -1.3701 & -0.26848 & -0.26298 \\ -1.7001 & -4.0727 & -0.74026 & 3.0177 & -0.79445 & -2.3508 \\ 0.68063 & -1.82 & 2.5792 & 5.3129 & -0.30332 & 0.45725 \\ -3.6926 & -0.09014 & 0.18516 & 0.96 & 1.5596 & -1.8268 \\ -0.51557 & 0.51128 & 0.97846 & -1.087 & 2.7065 & 0.60245 \end{bmatrix}$$

$$Weight_{output} = [4.543 \quad -1.0024 \quad 2.7471 \quad 1.2239 \quad -2.762]$$

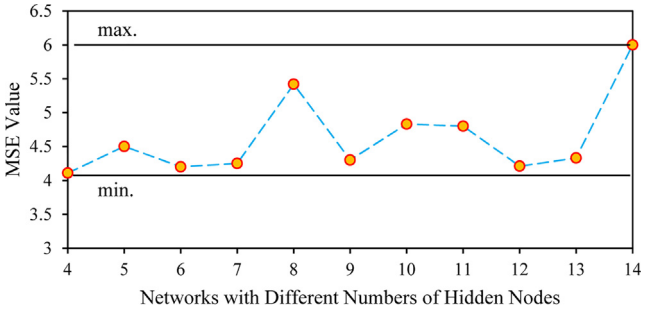

Fig. 3. MSE value versus various number of neurons in hidden layer.

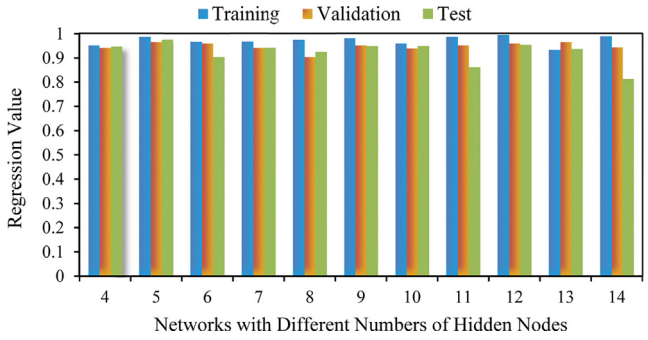

Fig. 4. Regression values versus number of neurons in hidden layer.

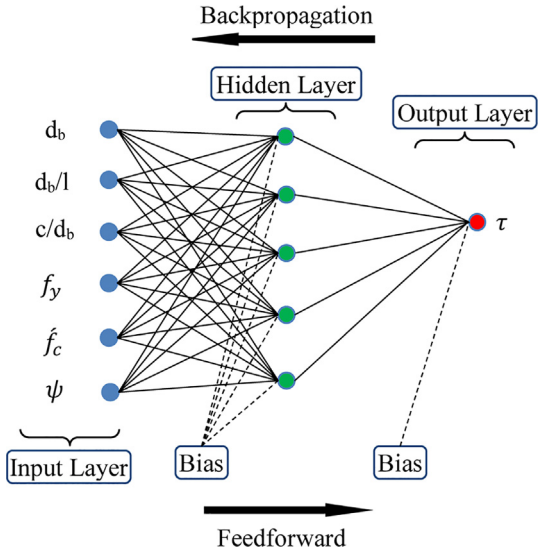

Fig. 5. Schematic diagram of proposed ANNs model.

$$Bias_{hidden}{}^{T} = [0.60654 \quad 0.34286 \quad 0.19363 \quad 0.49809 \quad 2.5619]$$

$$Bias_{output} = [0.0107]$$

4.3. Comparison of proposed model with experimental data

To check the precision of the proposed model, a comparison between simulated data and results of experimental results is carried out. The comparison is made based on the test data set using mean squared error (MSE) and correlation coefficient (R). The mean absolute error between targets and outputs of the proposed approach was equal to 15%. The comparison results and performance curve of the best ANN model based on the test dataset are illustrated in Fig. 6.

The performance curve revealed that the proposed model has appropriate performance in various corrosion levels, and the trend of bond stress was achieved with the least complications. In addi-

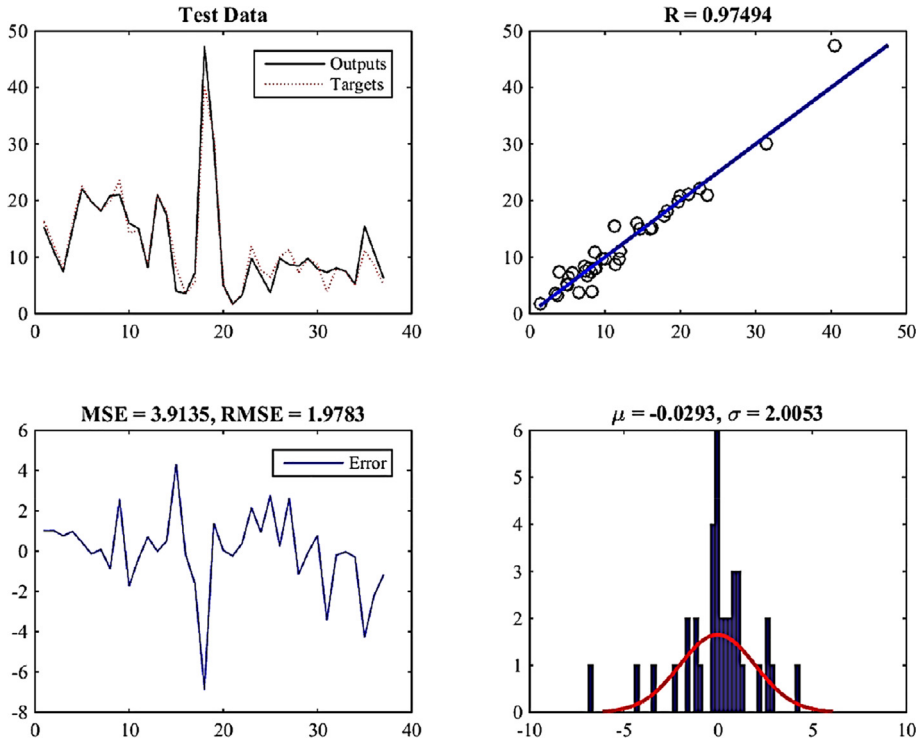

Fig. 6. Performance of the best network.

tion, the error bar used to demonstrate the distribution of error. The results revealed that the major part of the test data had less than five percent error compared to the test data.

5. Conclusion

This study proposed a prediction method for calculating the bond stress of corroded steel reinforcing bar based on the collected data of experimental investigations from published papers by means of artificial neural networks. The considered steel bars in database were deformed bars and it is assumed that the corrosion occurred after casting of concrete. The loading condition was monotonic tension where the results obtained from pull-out test. The Levenberg–Marquardt algorithm was utilized for training procedure. The ANN approach with five number of nodes in hidden layer was chosen as the best one based on considered criteria. The MAE of optimum network was equal to 15%, which shows appropriate ability to simulate experimented data on the safe side for most specimens. The present model could be used in the reliability assessment of corroded concrete structures in a corrosive environment.

CRediT authorship contribution statement

Masoud Ahmadi: Conceptualization, Data curation, Methodology, Software, Validation, Writing - original draft, Writing - review & editing. **Ali Kheyroddin:** Conceptualization, Methodology, Validation, Resources, Supervision, Project administration. **Mahdi Kioumarsi:** Resources, Methodology, Supervision, Writing - original draft, Writing - review & editing.

Declaration of Competing Interest

The authors declare that they have no known competing financial interests or personal relationships that could have appeared to influence the work reported in this paper.

References

[1] A.H. Nilson, D. Darwin, C.W. Dolan, Design of Concrete Structures, 13th ed,., McGraw-Hill Higher Education, 2004.
[2] A. Benenato, B. Ferracuti, S. Imperatore, M. Kioumarsi, Bond strength of RC elements with consideration of corrosion: An experimental survey, in: AIP Conf. Proc., AIP Publishing LLC, 2020: p. 240010.
[3] M. Kioumarsi, M.A.N. Hendriks, J. Kohler, M.R. Geiker, The effect of interference of corrosion pits on the failure probability of a reinforced concrete beam, Eng. Struct. 114 (2016) 113–121.
[4] L. Chung, J.-H.-J. Kim, S.-T. Yi, Bond strength prediction for reinforced concrete members with highly corroded reinforcing bars, Cem. Concr. Compos. 30 (2008) 603–611.
[5] M. Kioumarsi, A. Benenato, B. Ferracuti, S. Imperatore, Residual flexural capacity of corroded prestressed reinforced concrete beams, Metal 11 (3) (2021) 442, https://doi.org/10.3390/met11030442.
[6] K. Lundgren, P. Kettil, K.Z. Hanjari, H. Schlune, A.S.S. Roman, Analytical model for the bond-slip behaviour of corroded ribbed reinforcement, Struct. Infrastruct. Eng. 8 (2012) 157–169.
[7] P. Inci, C. Goksu, A. Ilki, N. Kumbasar, Effects of reinforcement corrosion on the performance of RC frame buildings subjected to seismic actions, J. Perform. Constr. Facil. 27 (2013) 683–696.
[8] C. Jiang, Y.-F. Wu, M.-J. Dai, Degradation of steel-to-concrete bond due to corrosion, Constr. Build. Mater. 158 (2018) 1073–1080.
[9] A. Bossio, S. Imperatore, M. Kioumarsi, Ultimate flexural capacity of reinforced concrete elements damaged by corrosion, Buildings 9 (2019) 160.
[10] M. Kioumarsi, M.A.N. Hendriks, M. Geiker, Failure probability of a corroded beam with interference effect of localised corrosion, Nord. Concr. 53 (2015) 39.
[11] K. Zandi Hanjari, P. Kettil, K. Lundgren, Analysis of mechanical behavior of corroded reinforced concrete structures, ACI Struct. J. 108 (2011) 532–541.
[12] M. Kioumarsi, M.A. Hendriks, M.R. Geiker, Quantification of the interference of localised corrosion on adjacent reinforcement bars in a concrete beam in bending, Nord. Concr. Res. 49 (2014) 39–57.
[13] M. Kioumarsi, M.A. Hendriks, M.R. Geiker, Interference of localised corrosion in adjacent reinforcement bar of a beam in bending, Concr. Innov. Conf. (2014).
[14] S. Bahl, A.K. Bagha, Finite element modeling and simulation of the fiber–matrix interface in fiber reinforced metal matrix composites, Mater. Today Proc. 39 (P1) (2021) 70–76.
[15] D. Guleria, H. Kumar, S. Sehgal, S. Singh, Impact of armor-perforating projectile on a bullet-resistant silicon-carbide-graphene composite through finite element method, Emerg. Trends Mech. Eng., Springer (2021) 3–18.
[16] M.K. Saini, A.K. Bagha, S. Kumar, S. Bahl, Finite element analysis for predicting the vibration characteristics of natural fiber reinforced epoxy composites, Mater. Today Proc. 41 (P2) (2021) 223–227.
[17] A.K. Bagha, S. Bahl, Strain energy and finite element analysis to predict the mechanical properties of vapor grown carbon fiber reinforced polypropylene nanocomposites, Mater. Today Proc. 41 (P2) (2021) 265–268.

[18] A. Kandiri, F. Sartipi, M. Kioumarsi, Predicting compressive strength of concrete containing recycled aggregate using modified ANN with different optimization algorithms, Appl. Sci. 11 (2021) 485.
[19] M. Kioumarsi, F. Azarhomayun, M. Haji, M. Shekarchi, Effect of shrinkage reducing admixture on drying shrinkage of concrete with different w/c ratios, Materials (Basel) 13 (2020) 5721.
[20] L. Taerwe, S. Matthys, Fib model code for concrete structures 2010, Ernst & Sohn, Wiley, 2013.
[21] Y.-F. Wu, X.-M. Zhao, Unified bond stress–slip model for reinforced concrete, J. Struct. Eng. 139 (2013) 1951–1962.
[22] D. Coronelli, Corrosion cracking and bond strength modeling for corroded bars in reinforced concrete, Struct. J. 99 (2002) 267–276.
[23] H.-S. Lee, T. Noguchi, F. Tomosawa, Evaluation of the bond properties between concrete and reinforcement as a function of the degree of reinforcement corrosion, Cem. Concr. Res. 32 (2002) 1313–1318.
[24] J.G. Cabrera, Deterioration of concrete due to reinforcement steel corrosion, Cem. Concr. Compos. 18 (1996) 47–59.
[25] X. Wang, X. Liu, Modeling bond strength of corroded reinforcement without stirrups, Cem. Concr. Res. 34 (2004) 1331–1339.
[26] F.I. du Béton, Bond of reinforcement in concrete: state-of-art report, Bulletin 10 (2000) 160–167.
[27] K.D. Stanish, Corrosion effects on bond strength in reinforced concrete, (1999).
[28] M. Blomfors, K. Zandi, K. Lundgren, D. Coronelli, Engineering bond model for corroded reinforcement, Eng. Struct. 156 (2018) 394–410.
[29] B. 65, Fib Model Code for Concrete Structures, 2010.
[30] Y. Auyeung, P. Balaguru, L. Chung, Bond behavior of corroded reinforcement bars, Mater. J. 97 (2000) 214–220.
[31] C. Fang, K. Lundgren, L. Chen, C. Zhu, Corrosion influence on bond in reinforced concrete, Cem. Concr. Res. 34 (2004) 2159–2167.
[32] J.G. Cabrera, P. Ghoddoussi, The effect of reinforcement corrosion on the strength of the steel/concrete bond, in: Int. Conf., Bond Concr. Res. to Pr., 1992: pp. 10–11.
[33] S. Ng, B.C. Craig, K.A. Soudki, Effects of FRP wrapping on the bond strength of corroded steel reinforcing bars, in: 2nd Mater. Spec. Conf. Can. Soc. Civ. Eng. Montr. Canada, 2002: pp. 1–9.
[34] D.W. Law, D. Tang, T.K.C. Molyneaux, R. Gravina, Impact of crack width on bond: confined and unconfined rebar, Mater. Struct. 44 (2011) 1287–1296.
[35] G.J. Al-Sulaimani, M. Kaleemullah, I.A. Basunbul, Influence of corrosion and cracking on bond behavior and strength of reinforced concrete members, Struct. J. 87 (1990) 220–231.
[36] S. Coccia, S. Imperatore, Z. Rinaldi, Influence of corrosion on the bond strength of steel rebars in concrete, Mater. Struct. 49 (2016) 537–551.
[37] H. Shima, Local bond stress-slip relationship of corroded steel bars embedded in concrete, in: Proceeding Third Int. Symp. Bond Concr. Budapest, 2002: pp. 153–158.
[38] G. Horrigmoe, I. Sæther, R. Antonsen, B. Arntsen, Laboratory investigations of steel bar corrosion in concrete, Sustain. Bridg. WP3 D (2007) 3.
[39] M. Ahmadi, H. Naderpour, A. Kheyroddin, Utilization of artificial neural networks to prediction of the capacity of CCFT short columns subject to short term axial load, Arch. Civ. Mech. Eng. 14 (2014) 510–517, https://doi.org/10.1016/j.acme.2014.01.006.
[40] M. Ahmadi, H. Naderpour, A. Kheyroddin, ANN model for predicting the compressive strength of circular steel-confined concrete, Int. J. Civ. Eng. 15 (2017) 213–221, https://doi.org/10.1007/s40999-016-0096-0.
[41] M.E. Jamkhaneh, M. Ahmadi, P. Sadeghian, Simplified relations for confinement factors of partially and highly confined areas of concrete in partially encased composite columns, Eng. Struct. 208 (2020) 110303.
[42] M. Ahmadi, A. Kheyroddin, A. Dalvand, M. Kioumarsi, New empirical approach for determining nominal shear capacity of steel fiber reinforced concrete beams, Constr. Build. Mater. 234 (2020) 117293.
[43] A. Kheyroddin, M. Ahmadi, M. Kioumarsi, Using Intelligent System Approach for Shear Strength Forecasting of Steel Fiber-Reinforced Concrete Beams, in: SynerCrete'18 Interdiscip. Approaches Cem. Mater. Struct. Concr. Synerg. Expert. Bridg. Scales Sp. Time., 2018.
[44] H. Naderpour, O. Poursaeidi, M. Ahmadi, Shear resistance prediction of concrete beams reinforced by FRP bars using artificial neural networks, Measurement 126 (2018) 299–308.
[45] M. Ahmadi, H. Naderpour, A. Kheyroddin, A. Gandomi, Seismic failure probability and vulnerability assessment of steel-concrete composite structures, Period. Polytech. Civ. Eng. 61 (2017) 939–950, https://doi.org/10.3311/PPci.10548.
[46] M. Shariati, M.S. Mafipour, B. Ghahremani, F. Azarhomayun, M. Ahmadi, N.T. Trung, A. Shariati, A novel hybrid extreme learning machine–grey wolf optimizer (ELM-GWO) model to predict compressive strength of concrete with partial replacements for cement, Eng. Comput. 1–23 (2020).
[47] M. Shariati, M.S. Mafipour, P. Mehrabi, M. Ahmadi, K. Wakil, N.T. Trung, A. Toghroli, Prediction of concrete strength in presence of furnace slag and fly ash using Hybrid ANN-GA (Artificial Neural Network-Genetic Algorithm), Smart Struct. Syst. 25 (2020) 183–195.
[48] M.H. Beale, M.T. Hagan, H.B. Demuth, Neural network toolbox, User's Guid. MathWorks. 2 (2010) 77–81.